Investigation on shipboard power quality on cruise ships under high penetration of power converters

Federico Graffione[a], Francesco Ghio[a], Marco Gallo[a], Fabio D'Agostino[a], Andrea Rudan[b], Federico Silvestro[a*]

[a]*University of Genova, Italy;* [b]*Carnival Corporation, Italy*
*Corresponding author. Email: federico.silvestro@unige.it

Synopsis

The maritime industry is undergoing a significant transformation with the integration of advanced power electronics and converter technologies onboard cruise ships. This work explores the effects of power converter integration on shipboard power quality, particularly in cruise vessels that depend heavily on these converters for efficient power conversion. The study proposes a preliminary investigation of the potential challenges arising from the complex interplay of power electronic devices, including variable frequency drives, rectifiers, and inverters, with the ship's power distribution grid. A comprehensive measurement campaign is conducted onboard representative cruise ships, utilizing advanced monitoring equipment to capture power quality indexes related to different power systems and conversion architecture. The primary objectives of this investigation are to assess power quality indexes and to develop models for analyzing and validating real measurement data. Two similar cruise ships, each equipped with different technologies for driving synchronous propulsion motors, were used as case studies. Through data analysis and ETAP modeling, the research compares the performance and power quality impacts of these technologies under various operational conditions. The findings reveal distinct total harmonic distortion of voltage behaviours for the two ships, highlighting the varying effects of synchro-converters and cyclo-converters on power quality during port and navigation conditions. The study emphasizes the importance of maintaining a stable and high-quality power supply in the maritime environment, and provides insights into the implications of power quality issues on the performance of onboard equipment.

Keywords: Power Quality, Shipboard Power System, Total Harmonic Distortion, All Electric Ship, Harmonic Load Flow.

1 Introduction

The electrification of ships has led to an increasingly widespread presence of power electronics and converters, particularly on All Electric Ship (AES). These technologies play a crucial role when there is a necessity to generate, distribute electrical power. Furthermore, to improve the energy efficiency of the ship, Direct Current (DC) energy sources such as Fuel Cell (FC) and Battery Energy Storage System (BESS) are progressively being implemented Gallo et al. (2023). These types of resources need to be interfaced to the ship's grid using converters. The presence of this power electronics equipment introduces power quality issues Barros and Diego (2016).

The definition of power quality is given by International Electrotechnical Commission (2024): *"characteristics of the electric current, voltage and frequency at a given point in an electric power system, evaluated against a set of reference technical parameters"*.

International standards, specifically related to shipboard power system applications, define both the typical operating conditions and the reference technical parameters. These deviations are considered within the power quality assessment and are measured using various indices and measurement methods IEEE (2009); International Association of Classification Societies (IACS) (2019); IEEE (2014).

Among the various metrics used to evaluate power quality, harmonic content is one of the key indicators. Harmonics, which are integer multiples of the power system frequency, are created by non-linear loads that distort

voltage waveforms and impact the entire power system. Harmonics are usually related to the presence of non-linear loads, such as propulsion motors and drives. The widespread use of power converters in marine applications, like propulsion and pumps, has led to non-linear loading constituting up to 80% of the generation capacity on modern vessels Kůs et al..

The limits defined by international organizations and marine classification societies, such as IEC, IEEE, DNV, ABS, and LRS, specify the allowable voltage harmonic distortion for shipboard electrical installations under all operating conditions. Standards refer to limits for Total Harmonic Distortion (THD), which measure the distortion caused by harmonics as a percentage of the fundamental frequency in voltage or current waveforms Milankov and Radić (2014). THD can be measured for both the voltage and the current. The THD voltage limit ranges from 5% to 8%, depending on the standard considered Barros and Diego (2016). The single harmonic limit ranges from 1.5% to 3%.

In the existing literature, authors have proposed different approaches to analyze and address power quality issues. In Tsvetanov et al. (2023b), an experimental setup is presented to evaluate the performance of an autonomous Shipboard Power System (SPS) in terms of THD. In Liu et al. (2018), an investigation on the power quality assessment onboard ship is suggested. The analysis shows that the effect of voltage unbalance and distortions in the SPS must be taken into account, particularly when differences on critical grid parameters under balanced and unbalanced are quite important. In Rigogiannis et al. (2023), power quality measurements on a ferry boat are presented. The analysis highlights the issue of high THD values associated with the power conditioning system. In Terriche et al. (2019), authors propose two open-loop algorithms to assess the harmonic distortion for short and long term preventive action stage on AES. In Mindykowski and Tarasiuk (2015), an analysis of the problem of electrical power quality and its impact in terms of safety is presented. The authors emphasize that ship classification societies should introduce requirements for the continuous monitoring of power quality in ship systems. In Crapse et al. (2007), a specific frequency-based power quality index is proposed to measure disturbances at different critical points within an electric ship power system.

Other studies investigate different solutions to manage the effects of power electronic devices on the electric grid. In Rahman et al. (2022), a distribution filtering solution is modelled and implemented, emphasizing the optimal placement of active filters primarily at higher voltage nodes. In Tsvetanov et al. (2023a), a static synchronous compensator is modelled to improve the power factor in autonomous SPS. In Semwal et al. (2022), an enhanced fractional least mean square is developed to improve the power quality in shipboard microgrids. In Li et al. (2017), a controllable inductive power filtering method is proposed. This method serves multiple purposes, including reducing the required installation space, suppressing harmonic currents, and damping harmonic resonance in the SPS. In Terriche et al. (2019), a combined structure of hybrid active power filter with parallel fixed capacitor-thyristor controlled reactor is proposed to compensate for the distortion and the sags of the voltage in SPS. In Liu et al. (2022), the authors introduce a shipboard power supply system that integrates transformers and filters. This setup ensures a harmonic-free power supply, benefiting stable operation and integrated optimization of compact, all-electric shipboard systems.

The proposed manuscript presents a methodology for analyzing and validating real measurement data collected from cruise ships under normal operating conditions. The primary goal is to analyse the power quality on the SPS. To verify the results derived from the data analysis, a model of the SPS is developed using the ETAP environment.

The paper is organized as follows: Section 2 introduces the analysis on the power quality measurements, Section 3 reports the development of the SPS model and non-linear loads behaviour, Section 4 presents model validation through the comparison with the real measurements, while conclusions are proposed in Section 5.

2 Power quality analysis in SPS

This study examines real power quality measurements taken from two cruise ships. The analysis is performed under specific assumptions using various correlation techniques. The primary metric for assessing power quality in this study is the voltage THD. This section describes the ships analyzed, the types of available data, and the analysis conducted. The two considered cruise ships are identified as Study Case 1 (SC1) and Study Case 2 (SC2). They fall into the category of mass-market cruises. The SPS of SC1 and SC2 is quite similar except for the type of propulsion drives, which are the main contributors to harmonic distortion.

2.1 Description of the SPS, for the SC1

Figure 1 presents the Medium Voltage (MV) single-line diagram of SC1. The generating resources of the ship are composed of six 14 MVA synchronous machines, driven by Diesel prime movers, connected to two main busbars at 11 kV.

Six 1720 kW asynchronous motors, used as manoeuvring thrusters, are directly connected (without intermediate speed control drive) to the main switchboard. These include three bow thrusters and three stern thrusters. Additionally, there are four Heat Ventilation and Air Conditioning (HVAC) compressors equipped with 1500 kW
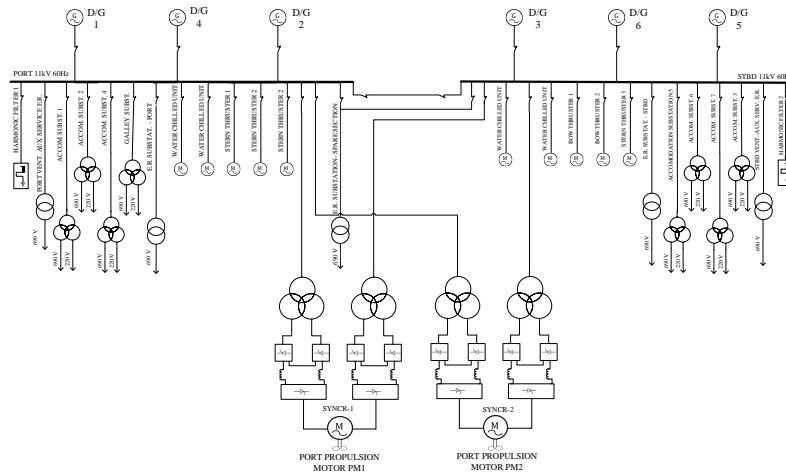
Figure 1: Shipboard Power System for SC1 cruise ship.

asynchronous motors. Transformers are used to supply Low Voltage (LV) busbars of hotel substations (on for each main vertical zones), the machinery auxiliary substations (divided into five substations), and the galley substation. In addition, the machinery auxiliary substations are further divided into two *Engine Room Ventilation Auxiliary Service*, two *Engine Room Substation* and one *Engine Room Substation - Spare Section*. There are two types of transformers: two-winding and three-winding. The three-winding transformer, composed of a primary winding and two secondary windings, allows supplying two different voltage levels. In this case, the two-winding transformers provide power to the machinery auxiliary substations, stepping down from 11 kV to 690 V. For the *Engine Room Ventilation Auxiliary Service*, these transformers have a rated apparent power of 2800 kVA, while for the *Engine Room Substation*, it is 3500 kVA. The hotel substations are powered by three-winding transformers with a rated apparent power of 1500 kVA, stepping down from 11 kV to 690 V and 220 V. Galley is supplied by a three-winding transformer with a rated apparent power of 2600 kVA, also stepping down from 11 kV to 690 V and 220 V.

The main propulsion service is provided by two Fixed Pitch Propeller (FPP) driven by two-windings synchronous machines, with a mechanical rated power of 21 MW. The electrical power system is provided through four 11/1.5/1.5 kV/kV/kV three-winding transformers, each rated at 13.4 MVA. The four transformers supply two synchroconverters, one for each propulsion motor. The synchroconverter is a power electronics component that realizes an Alternative Current (AC)-DC-AC conversion. It provides an output voltage with a variable frequency, so that the speed of the synchronous motor can be regulated

Finally, two double-tuned passive harmonic filters are connected to the MV busbar. These filters contain harmonic pollution, thus reducing the THD.

2.2 Description of the SPS, for the SC2

Figure 2 shows the single line diagram for the SC2. The generating resources of the ship are composed of four 16 MVA Diesel Generator (DG) and two 12 MVA DGs. These generators provide power at the MV busbar at 6.6 kV, 60 Hz. Similar to SC1, six manoeuvring thrusters with a power of 1720 kW are connected direct online to the main busbar. Additionally, there are four HVAC compressors with a power rating of 1570 kW.

The main propulsion system consists of two synchronous motors, each with a mechanical output power of 20 MW. Each motor drives a Controllable Pitch Propeller (CPP). Electrical power is supplied by four two-winding transformers that feed two cycloconverters. These devices are power electronics apparatuses that realize an AC-AC conversion, so that the synchronous motors' speed can be controlled through the regulation of the output voltage frequency.

2.3 Description of the available data

In the ships previously described, reported in Fig. 1 and in Fig. 2, active power data [kW] absorbed by the loads connected to the MV busbar are available. These measurements have been taken at the primary winding side on the transformers that separate the main switchboard from the secondary distribution grid. For installations not served by transformers, such as manoeuvring thrusters and HVAC compressors, measurements have been taken directly at the machine terminals. For the power plant, active and reactive power, current, voltage, and current and voltage THD are available. Finally, regarding propulsion motors, there are two types of data: active absorbed power
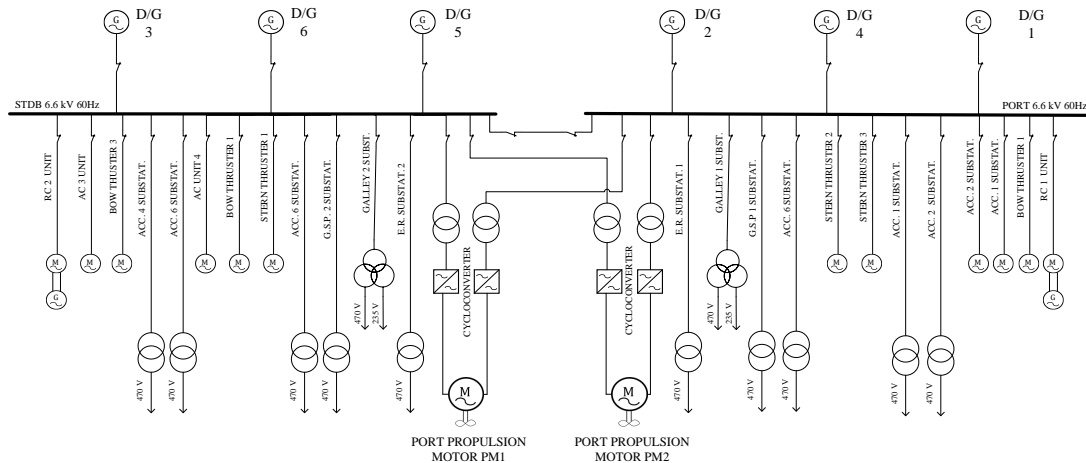
Figure 2: Shipboard Power System for SC2 cruise ship.

data from synchronous propulsion motors and active absorbed power from three-winding propulsion transformers. Figure 3 shows the location of the measurement units.
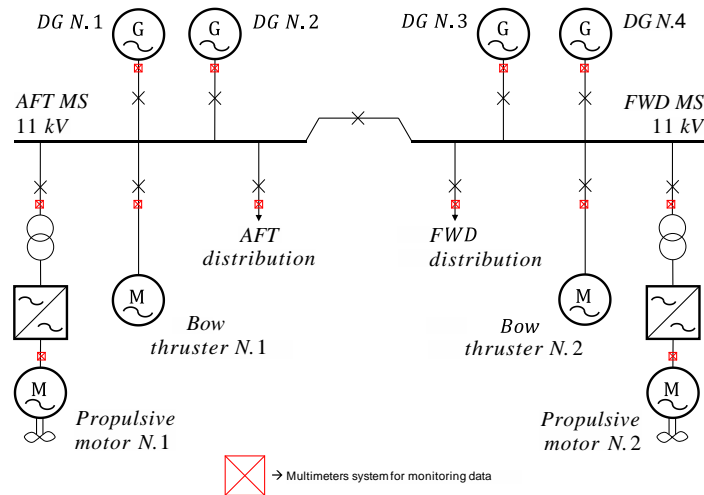
Figure 3: Notional arrangement diagram of multi-meters in the onboard electrical system.

The two ships operate on commercial cruise routes, typically spending the day in port, and sailing during the night.

Based on the power output from the onboard SPS, which varies with operational conditions and is primarily dependent on the sailing speed for SC1, we assume that:

- When it's in port (speed of 0 kn), the number of operating DGs is 1 to a maximum of 2, with a total active power output of approximately 8-10 MW, and peaks reaching 11 MW when 2 DG are active, with a mean cosphi = 0,87;

- During medium-speed navigation (between 8-13 kn), 2 DGs are required, collectively providing active power between 12-16,5 MW, with a mean cosphi = 0,80;

- For cruising speeds (18-21 kn), 3 DGs are needed, delivering a combined active power output of 27-37 MW, with a mean cosphi = 0,88. Peaks up to 46 MW are observed to achieve speeds around 23 knots, maybe in rough sea condition.

For SC2 it can be observed:

- When it's in port (speed of 0 kn), the number of operating DGs is 1, with a total active power output of approximately 6-7 MW, with a mean cosphi = 0,85, and peaks reaching 7,5 MW;

- During medium-speed navigation (between 8-13 kn), 2 DGs are required, collectively providing active power between 11-16 MW, with a mean cosphi = 0,61;

- For cruising speeds (18-22 kn), 4 DGs are needed, delivering a combined active power output of 25-35 MW, with a mean cosphi = 0,72. A peak of up to 41,5 MW is observed with 5 DGs active, presumably while navigating at a speed of approximately 20,4 kn, likely against adverse wind and current conditions or challenging marine weather.

The cubic relationships between the speed of the ship and the active power absorbed by the main propulsion, are shown in Fig. 4. These curves are obtained from measurements of active electrical power absorbed [MW] by the two synchronous propulsion motors, for both ships.
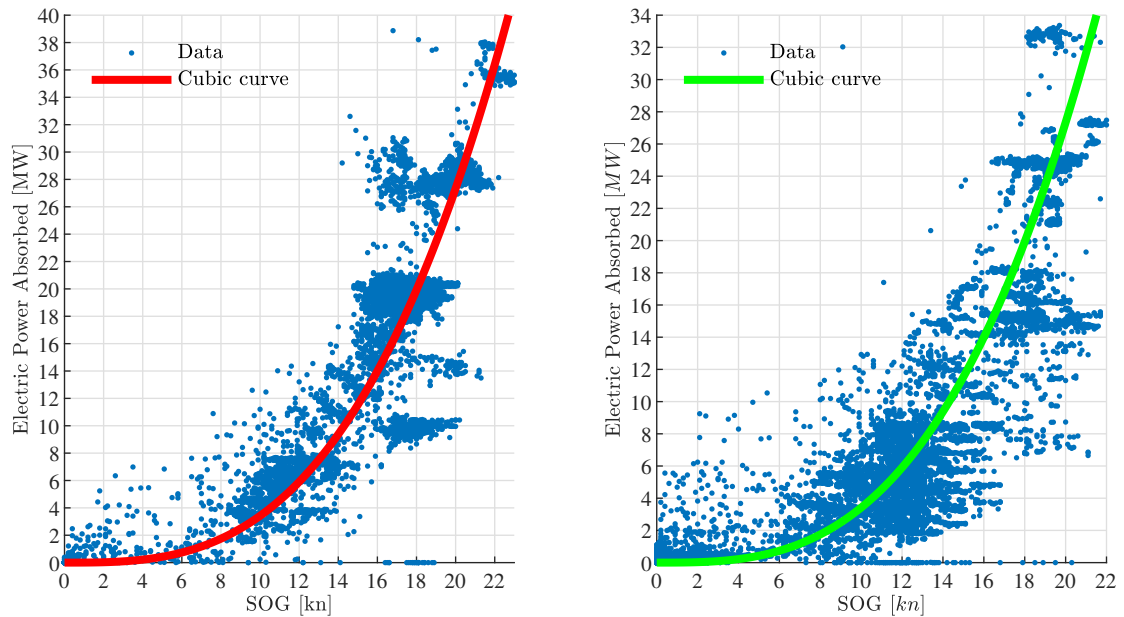
Figure 4: Cubic relationship fitting for SC1 (*left*), and for SC2 (*right*)

2.4 Analysis of Onboard Ship Measurement Data

The objective is to investigate the correlations between the active power absorbed from onboard electrical loads and the THD_V.

The initial step of the analysis involves categorizing the electrical load components divided into:

- Maneuvering thruster loads;

- HVAC compressors loads;

- Hotel substations loads;

- Engine auxiliary substations loads;

- Galley substations loads;

- Main propulsion loads.

Correlation analysis is performed. Pearson correlation coefficients are calculated for all pairs of input variables. A Pearson coefficient close to 1 indicates a tendency toward proportional and linear behavior in the data, while a coefficient near -1 suggests an inverse proportional relationship. Correlation is typically considered significant when greater than 70% Meghanathan (2016).

Measurements of the THD_V are taken by meters installed on the generator incoming cubicle, between the DG alternator and the MV busbar. Therefore, the number of meters corresponds to the number of DGs, as do the THD_V values. Simplifying by calculating an average value is appropriate since the observed values are relatively similar. Calculating an average value makes it easier to visualize and appreciate the behavior based on operational conditions, the number of DGs in operation, the electrical power generated by the plant, and the power absorbed by the onboard electrical loads.

Item 1	Item 2	SC1	SC2
HVAC compressor	THD_V	-0.15	-0.05
Maneuvering thruster	THD_V	0.23	-0.20
Hotel substation	THD_V	0.13	0.11
Galley	THD_V	0.14	0.02
Main propulsion	THD_V	-0.82	0.65
Engine auxiliary substation	THD_V	-0.65	0.52
Electric power supplied by DG	Main propulsion	0.97	0.97

Table I: Summary Table of Correlation Research

The Table I provides a summary of the correlation research between load categories for both case studies. The only load category strongly correlated with the variation in average THD is the main propulsion. Auxiliary machine substations also show a correlation because some loads support the main propulsion and therefore align with the load demand of the main synchronous motors. In Fig. 5, the correlation value between individual substations and the mean THD_V are represented, to identify which substation is most strongly correlated with the increase in load absorbed by the propulsion.

Figure 5 shows that for SC1 substations D, E, and F are most correlated with the variation of average THD_V, while for SC2 substations A and B exhibit this correlation.

Table I indicates a correlation between the power supplied by DGs and the electric power absorbed by the main propulsion, with a correlation coefficient of approximately 1, as these two quantities are of similar magnitude. Therefore, the primary variation in load supplied by the SPS is due to the load demand or reduction of absorption by the main propulsion.

Furthermore, in the correlation between synchronous propulsion motors power absorbed and the mean THD_V, there are different signs in the Pearson correlation coefficient between SC1 and SC2. For SC1, the correlation is negative, indicating that as the active power absorbed by the propulsion increases, the mean THD_V decreases. Conversely, for SC2, the correlation is positive, meaning that as the active power absorbed by the propulsion increases, the mean THD_V also increases.

In Fig. 6 and in Fig. 7, a typical daily profile in terms of active generated power, speed, and mean THD_V is shown. From the speed profile, it is possible to distinguish two main operational conditions, port and navigation.

For SC1, the mean THD_V decreases with increasing speed and, consequently, the active power absorbed by propulsion. In the other hand, for SC2, the opposite occurs. In SC1, there is a transition from a mean THD_V value ranging from approximately 4-4.5 (port condition) to 1.7-1.8 (navigation condition). Meanwhile, for SC2, there is

(a) SC1   (b) SC2
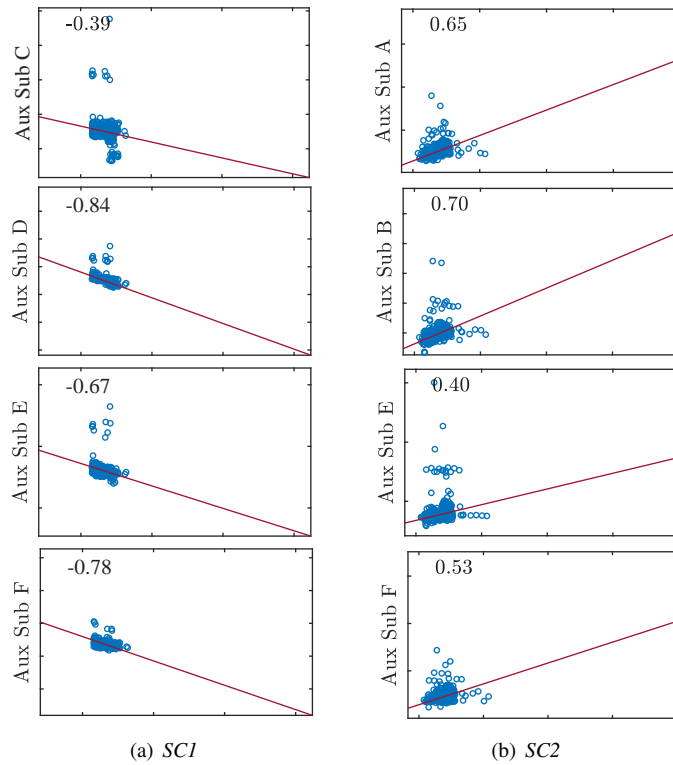
Figure 5: Correlation between Engine auxiliary and mean THD_V for both study case

a transition from mean THD_V around 2.9-3.2 (port condition) to 7.3-10.3 (navigation condition). The range within which THD_V varies for SC2 depends on the navigation speed; as speed increases, the mean THD_V also increases.
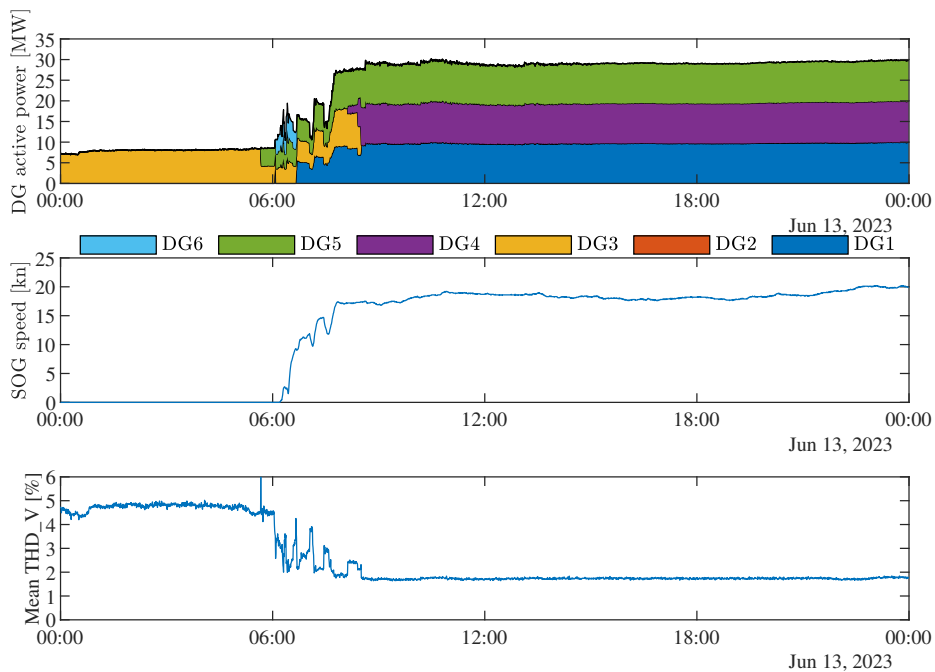
Figure 6: DG electrical power supplied, Speed Over Ground (SOG) and mean THD_V for SC1.

As previously mentioned, the two units have different technologies for driving synchronous propulsion motors. SC1 is equipped with a synchroconverter, while SC2 has a cycloconverter. The main difference in terms of har-
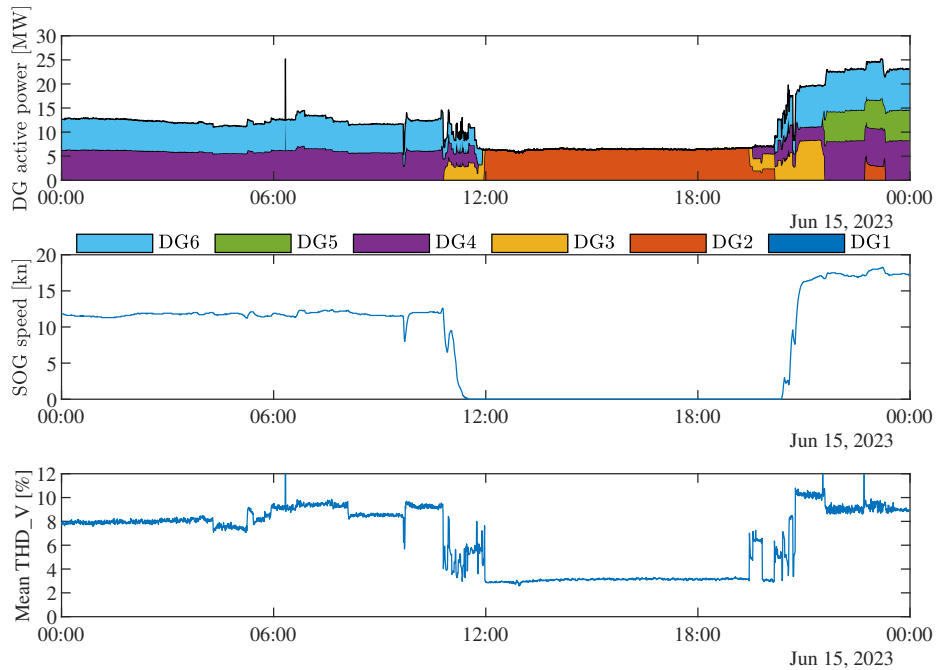
Figure 7: DG electrical power supplied, SOG and mean THD$_V$ for SC2.

monic pollution in the onboard grid is due to the fact that SC1 is equipped with two double-tuned passive harmonic filters (one for each busbar), whereas SC2 is not. As we will see in the following paragraphs, passive harmonic filters are connected to the grid when more than one DG is in operation. For SC1, this occurs during navigation, as typically only one DG is operational during port conditions.

3 Modeling of the integrated SPS

Starting from the data provided for the SPS of the SC1 and to validate the THD$_V$ measurements taken, a model is developed in ETAP environment. Specifically, the following assumptions are considered: the impedance of the cables is negligible compared to transformers and passive harmonic filters, the power factor of the substations is an input parameter, and the electrical loads of the substations are modelled as static loads. Part of the latter are considered as non-linear loads that inject harmonics according to the ideal current generator model with a certain injection profile. This was done by assuming the injection profile of the possible installed converters. Furthermore, synchronous generators and induction motors are modelled using the specific ETAP model component.

The model realization can be summarized in the following steps:

- Identification of operating conditions under steady-state conditions;

- Modeling the SPS in ETAP environment for the considered operating conditions;

- Performing Load Flow calculation;

- Performing recursive Harmonic Load Flow calculation to estimate the harmonic injection that match with real data measurements. Achieve convergence between the THD voltage value of the model and the real data measurements, by varying the percentage of loads under the converter until determining the amount of load injecting harmonics from the substations;

- Cross-validate the model results through the comparison with other operating condition related measurements.

3.1 Determining operating conditions

The load produced by the DG and the number of them in operation have been plotted, identifying conditions that can be defined as recursive over time regarding the THD$_V$ and the loads involved. It was noted:

- Case of ship in harbour $\rightarrow$ THD$_V \cong 4.30\%$;

- Case of ship in navigation $\rightarrow$ THD$_V \cong 1.7 - 1.8\%$.

Two points in time have been set under steady-state conditions, and the corresponding values of the electrical grid measurements have been assumed:

- Case of ship in harbour $\rightarrow$ 18/06/23 00:15 (UTC);

- Case of ship in navigation $\rightarrow$ 25/06/23 10:12 (UTC).
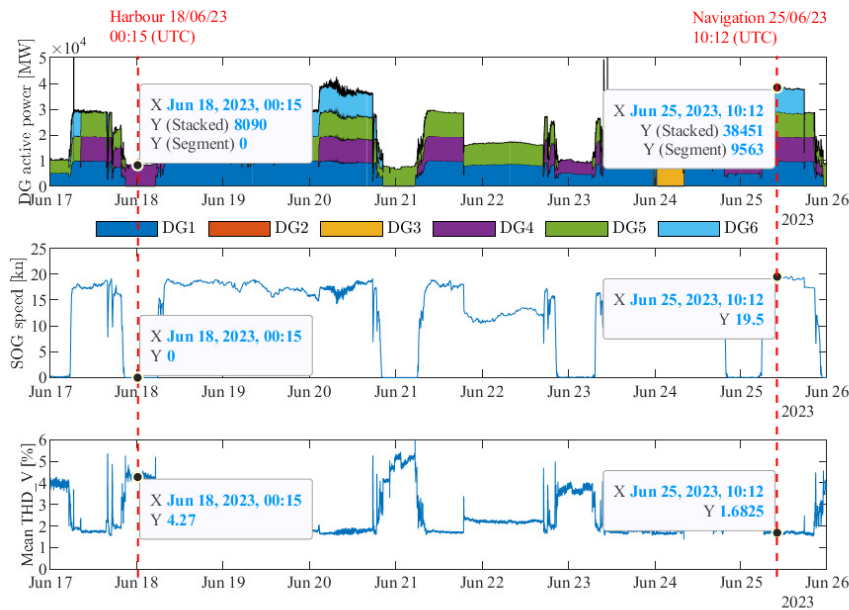
Figure 8: Temporal signal of active power generated by the onboard station, SOG speed, and average THD$_V$.

3.2   Modeling with ETAP Load Flow and Harmonic Load Flow

The SPS model is developed in the ETAP (Electrical Transient Analyzer Program) environment using the datasheets of the components. In this environment, it is possible to perform load flow analysis and harmonic load flow analysis. With ETAP, it is possible to perform a harmonic analysis of the grid and study the harmonic spectrum of voltage and current in the grid. This is done by modeling a load or a component as a 'harmonic source' and this is accomplished through a specific section in the settings of each load. Additionally, it is possible to perform a 'frequency scan' which returns the impedance magnitude and angle, as seen from the main switchboard.

3.3   Modeling the Electrical System of SC1 in ETAP

The ETAP model used for the load flow and harmonic load flow is presented in Figure 9.

In this model, the different modeling methods concerning linear and nonlinear loads are distinguished to perform a harmonic load flow analysis. An example of the different models is shown in Fig. 10, where:

- Load (1): this load represents the case of an electric motor controlled by a VFD (Variable Frequency Drive). For simplicity, it has been represented as a static load injecting harmonics according to the type of load and technology involved;

- Load (2): this load represents the case of substations, which we consider as aggregated loads of linear and non-linear loads. These are modeled as two static loads, one of which injects harmonics. The percentage of the load that injects harmonics is determined during the model calibration phase, and the injection profile is based on the present components;

- Load (3): This load represents the case of a load that can be considered linear, such as an induction motor, which is modeled according to the ETAP reference model.
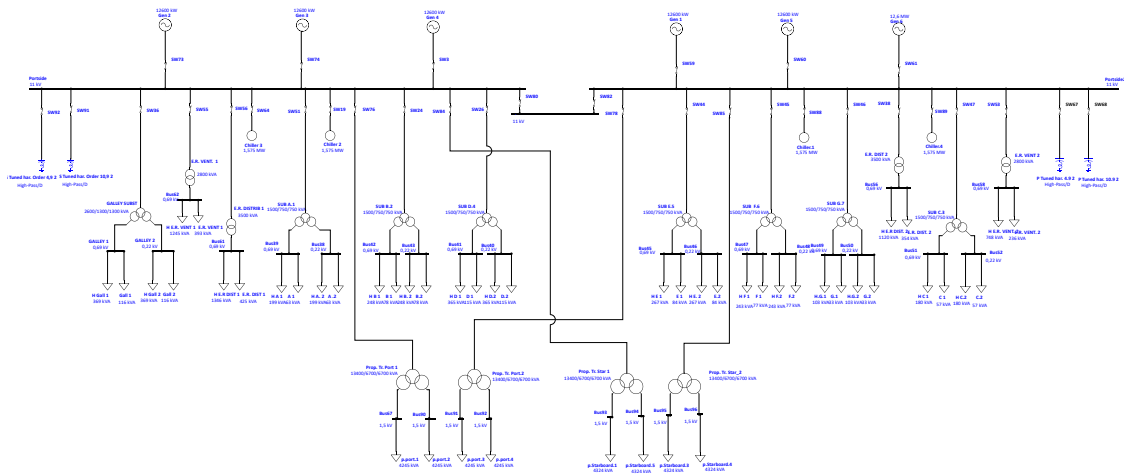
Figure 9: SPS ETAP model for harmonic analysis.
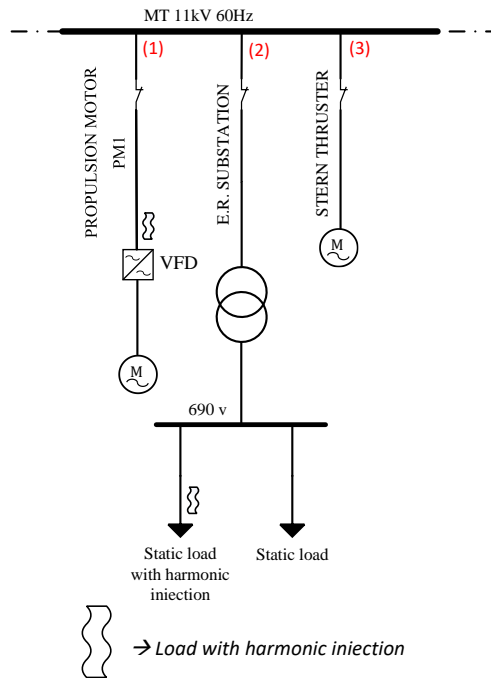
Figure 10: Example of modelling the different electric loads on ETAP.

The injection profiles assumed for the various electrical loads from the hotel substations, engine room substations, and propulsion are reported.

3.3.1 Propulsion Load

The harmonic injection profile for the propulsion loads is presented in the following figures and tables. This type of load is modelled as a (negative) current source with a defined harmonic spectrum, to represent a 24-pulse synchronous converter model, as shown in the following figures.

Harmonic Library	
Type:	Current Source
Manufacturer:	ABB
Model:	ACS600 6P
Phase Type:	Balanced

Table II: Harmonic injection model of the propulsive load

(a) *Current source injection waveform*

(b) *Current source injection spectrum*
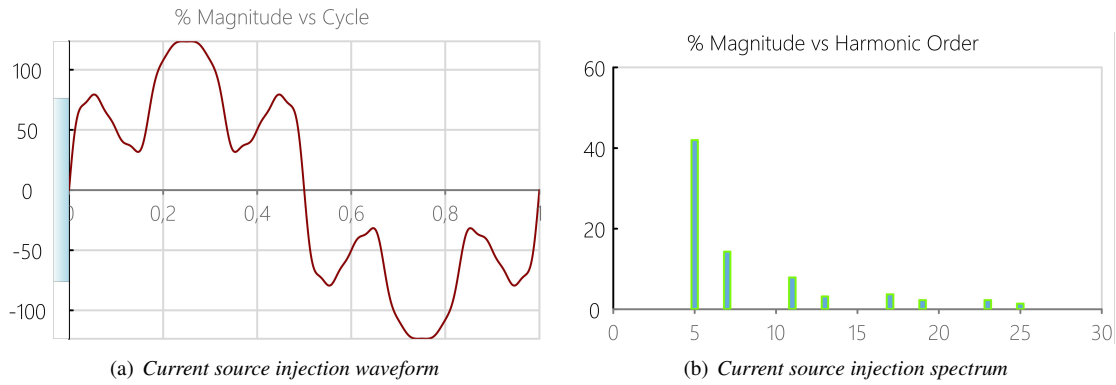
Figure 11: Injection form and spectrum ABB ACS600 6P
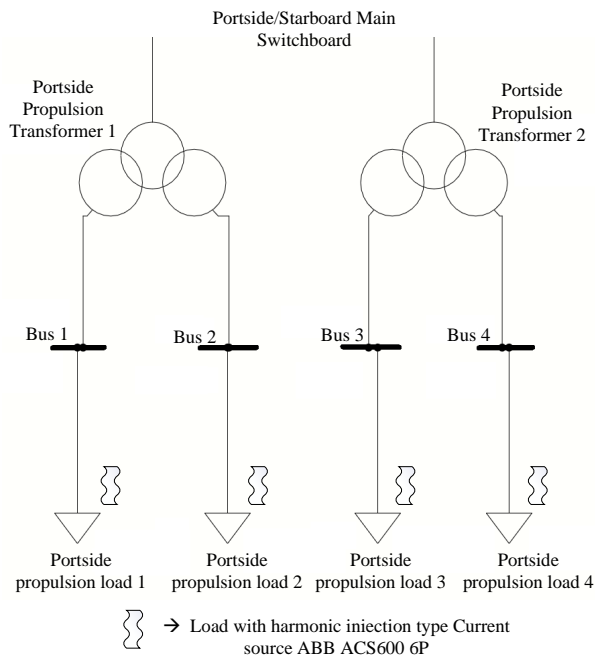
Figure 12: Model VFD 24 pulse in ETAP.

3.3.2 *Engine auxiliary substations load*

This type of load falls within the modeling of loads from the substations described earlier, so it is necessary to divide the load into two static loads. For the load injecting harmonics, it is considered that there are electrical components regulated by VFDs. The injection profile described in the following tables and figures is then assumed.

Harmonic Library	
Type:	Current Source
Manufacturer:	Rockwell
Model:	6-Pulse VFD
Phase Type:	Balanced

Table III: Harmonic injection model of the engine auxiliary substations load

3.3.3 *Hotel substations loads*

According to the real equipment information, a large part of each substation load (air conditioning) is supplied by a non-controllable 6-pulse rectifier. Therefore, an IEEE 6-pulse profile was used.

After several preliminary evaluations and calculations, the power factor of the electrical load from the substations has been assumed to be 0.92, while for the propulsion load, it was assumed to be 0.81.

(a) *Current source injection waveform*

(b) *Current source injection spectrum*
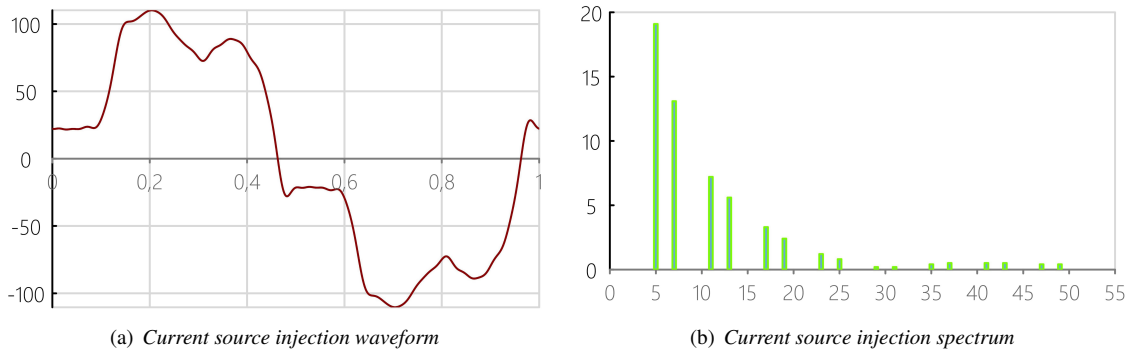
Figure 13: Injection form and spectrum 6-Pulse VFD

Harmonic Library	
Type:	Current Source
Manufacturer:	Typical IEEE
Model:	IEEE 6 Pulse
Phase Type:	Balanced

Table IV: Harmonic injection model of the hotel substations load

(a) *Current source injection waveform*

(b) *Current source injection spectrum*
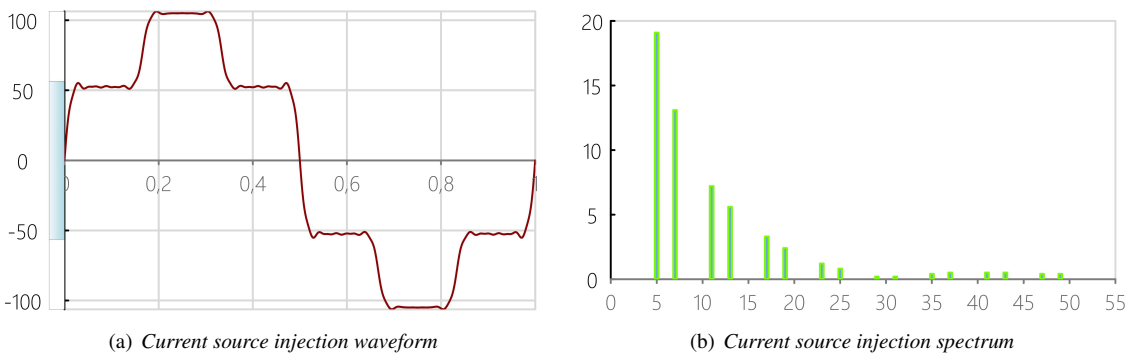
Figure 14: Injection form and spectrum IEEE 6 Pulse

4 Real data measurements validations

In this section, the results obtained from simulating the model using ETAP software are reported. Figure 15 shows the trend of THD_V on the main electrical panel as the percentage of harmonic load injection increases. It is noticeable how the trend is linear since, as the power under converters increases, it shows a linear correlation with the harmonic injection percentage.

These graphs provide the THD_V value obtained on the main panel as the portion of load subjected to converters increases. The results show that with approximately 76% of the load under converters and the assumed harmonic current injection profiles, the THD_V values match real measurements both when the ship is sailing and when it is in port.

4.1 Load flow results for harbour condition

In this section, Tables V and VI present the input data for the load flow related to the active and reactive power absorbed in the 'harbour' scenario. Another input is the voltage value on the main switchboard shown in Table VII, which is essential for achieving the adherence of the THD_V value of the harmonic load flow. Table VII also presents the load flow results in terms of current, active power, and reactive power supplied by the DG operating in the 'harbour' condition and the harmonic load flow results in terms of THD_V [%]. When data is absent in the table, it indicates components disconnected from the ship's power grid.

Figure16 presents the results, including the voltage waveform on the main switchboard, its spectrum, and the frequency scan, specifically the impedance angle and the impedance value related to the main switchboard.

(a) *Case "Harbour":*

(b) *Case "Navigation"*
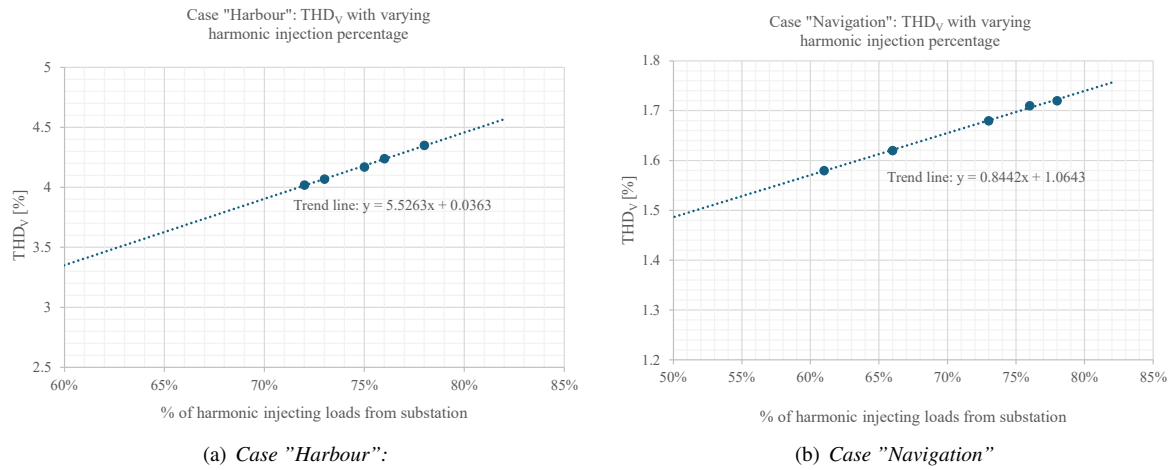
Figure 15: THD_V with varying harmonic injection percentage

Substation	ACTIVE ELECTRIC POWER ABSORBED [kW]	REACTIVE ELECTRIC POWER ABSORBED [kVAR]
Acc. n°1	494.6	217.8
Acc. n°2	644.1	286.4
Acc. n°3	427.2	187.3
Acc. n°4	843.8	380.2
Acc. n°5	712.5	318.3
Acc. n°6	618.6	274.6
Acc. n°7	271.9	118.0
Galley	625.9	274.4
E.R.Dist.1	1534.0	708.0
E.R.Vent.1	601.0	266.3
E.R.Dist.2	1242.0	564.8
E.R.Vent.2	609.1	270.0

Table V: Load Flow Substations Transformers SC1 Case "Harbour"

Measure Chiller	AC 1	AC 2	AC 3	AC 4
ACTIVE ELECTRIC POWER ABSORBED [kW]	-	701.3	-	-
REACTIVE ELECTRIC POWER ABSORBED [kVAR]	-	573.7	-	-

Table VI: Load Flow Chiller HVAC SC1 Case "Harbour"

Measure D/G	n°1	n°2	n°3	n°4	n°5	n°6
DG ACTIVE POWER [kW]	-	-	-	9326	-	-
DG CURRENT AVG [A]	-	-	-	543	-	-
DG REACTIVE POWER [kVAR]	-	-	-	4440	-	-
DG THD_V MAIN SWITCHBOARD [%]				4.21		
DG VOLTAGE AVG MAIN SWITCHBOARD [V]				10983		

Table VII: Load Flow Results DG SC1 Case "Harbour"

4.2 *Load flow results for navigation condition*

In this section, Tables VIII,IX,X andXI present the input data for the load flow related the active and reactive power absorbed in the 'navigation' scenario where, compared to the previous scenario, electrical loads from propulsion and harmonic filters in operation are added. The voltage value on the main switchboard is reported in Table XII. Table VII also presents the load flow results in terms of current, active power, and reactive power supplied by the DGs operating in the 'navigation' condition and the harmonic load flow results in terms of THD_V [%]. When data is absent in the table it indicates components disconnected from the ship's power grid.
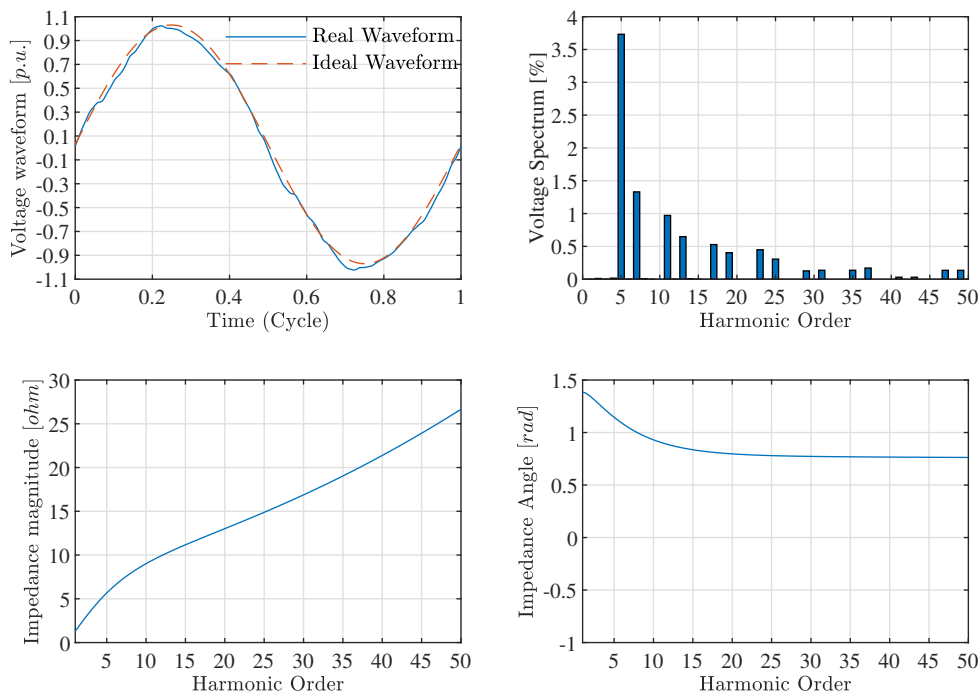
Figure 16: "Harbour" case

Substation	ACTIVE ELECTRIC POWER ABSORBED [kW]	REACTIVE ELECTRIC POWER ABSORBED [kVAR]
Acc. n°1	525.3	231.8
Acc. n°2	646.1	287.4
Acc. n°3	470.0	206.7
Acc. n°4	853.4	431.8
Acc. n°5	697.2	304.1
Acc. n°6	951.1	657.8
Acc. n°7	270.3	117.3
Galley	700.8	308.4
E.R.Dist.1	1782.0	797.2
E.R.Vent.1	1626.0	769.8
E.R.Dist.2	1481.0	304.1
E.R.Vent.2	993.2	451.5

Table VIII: Load Flow Substations Transformers SC1 Case "Navigation"

Measure Propulsion	PM 1	PM 2
ACTIVE ELECTRIC POWER ABSORBED [kW]	13050	13282
REACTIVE ELECTRIC POWER ABSORBED [kVAR]	8626	8790

Table IX: Load Flow Propulsion Transformers SC1 Case "Navigation"

Measure Chiller	AC 1	AC 2	AC 3	AC 4
ACTIVE ELECTRIC POWER ABSORBED [kW]	-	613.9	853.4	-
REACTIVE ELECTRIC POWER ABSORBED [kVAR]	-	518.4	658.0	-

Table X: Load Flow Chiller HVAC SC1 Case "Navigation"

Figure17 presents the results, including the voltage waveform on the main switchboard, its spectrum, and the

Measure Harmonic Filters	ACTIVE ELECTRIC POWER ABSORBED [kW]	REACTIVE ELECTRIC POWER ABSORBED [kVAR]
H.F. n°1 (4.9 th harmonic)	6.09	-2561
H.F. n°1 (10.9 th harmonic)	0.428	-2475
H.F. n°2 (4.9 th harmonic)	-	-
H.F. n°2 (10.9 th harmonic)	-	-

Table XI: Load Flow Harmonic Filters SC1 Case "Navigation"

Measure D/G	n°1	n°2	n°3	n°4	n°5	n°6
DG ACTIVE POWER [kW]	9604	-	-	9641	9643	9696
DG CURRENT AVG [A]	564.2	-	-	563.6	563.6	566.6
DG REACTIVE POWER [kVAR]	4720	-	-	4464	4610	4634
DG THD$_V$ MAIN SWITCHBOARD [%]	1.76					
DG VOLTAGE AVG MAIN SWITCHBOARD [V]	10950					

Table XII: Load Flow Results DG SC1 Case "Navigation"

frequency scan, specifically the impedance angle and the impedance value related to the main switchboard, where the operation of passive harmonic filters connected to the main switchboard can be observed.
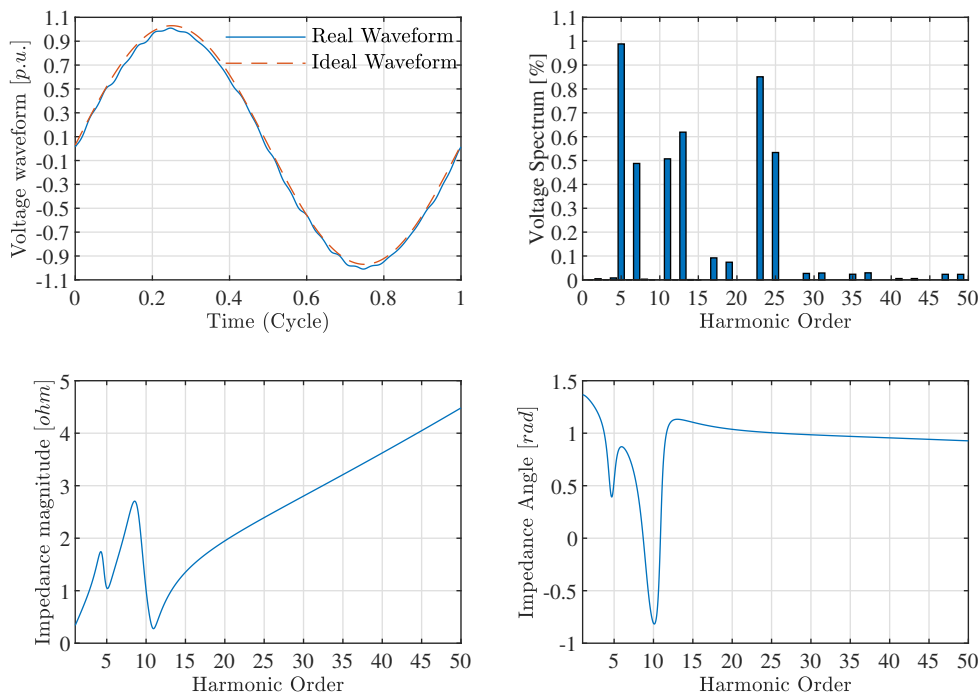
Figure 17: "Navigation" case

5   Conclusions and further research

This work has presented a methodology for analyzing and validating real measurement data collected from operating cruise ships, with the primary goal of studying power quality on the SPS. To verify the data analysis results, a model of the SPS is developed in the ETAP environment. Two similar cruise ships, equipped with different technologies for driving synchronous propulsion motors, were considered as case studies. SC1 is equipped with a synchro-converter, while SC2 uses a cyclo-converter. In port conditions, both units require only one DG to meet the electrical load. However, during navigation, at least two DGs are needed to meet the load demand, even at low speeds. The two units exhibit different THD_V behaviors under various operating conditions. In SC1, THD_V is higher during port operations and lower during navigation. Conversely, in SC2, THD_V is worse during navigation. The correlation between active power absorbed by the propulsion motors and THD_V shows a decreasing proportional correlation in SC1 and an increasing proportional correlation in SC2 (see Tab. I). An ETAP model was developed to compare and validate the data related to SC1, as more information was available regarding the SPS components. Following model calibration, load flow and harmonic load flow analyses were conducted. Comparing the frequency scans of 'harbour' and 'navigation' conditions revealed the impact of onboard passive harmonic filters on the power grid's impedance and power factor. In the 'navigation' condition, the filters operate at half their capacity, reducing system impedance at the tuning harmonics (4.9 and 10.9). This reduction aligns with the harmonic load flow results, showing decreased THD_V during navigation after the propulsion VFD operation. The ETAP model suggests that the lack of filtering action in port may cause THD_V values to approach the 8% threshold under steady-state conditions Mindykowski and Tarasiuk (2015). The ETAP model results, based on the active power values of electrical loads and voltage values at the main panel, show consistency between measured THD_V values and simulated results for the two steady-state conditions. This process verifies the data for SC1 and identifies the load magnitudes under converters and power electronics in various substations. Due to the complexity Future work will involve searching for harmonic injection profiles that yield specific THD_V values under various operating conditions, and filters configurations.

References

Barros, J., Diego, R.I., 2016. A review of measurement and analysis of electric power quality on shipboard power system networks. Renewable and Sustainable Energy Reviews 62, 665–672. doi:https://doi.org/10.1016/j.rser.2016.05.043.

Crapse, P., Wang, J., Abrams, J., Shin, Y.J., Dougal, R., 2007. Power quality assessment and management in an electric ship power system, in: IEEE Electric Ship Technologies Symposium, pp. 328–334. doi:10.1109/ESTS.2007.372106.

Gallo, M., Kaza, D., D'Agostino, F., Cavo, M., Zaccone, R., Silvestro, F., 2023. Power plant design for all-electric ships considering the assessment of carbon intensity indicator. Energy 283. doi:https://doi.org/10.1016/j.energy.2023.129091.

IEEE, 2009. IEEE Std 1159-2009. Recommended practice for monitoring electric power quality. IEEE Power and Energy Society .

IEEE, 2014. Ieee recommended practice and requirements for harmonic control in electric power systems. IEEE Std 519-2014 (Revision of IEEE Std 519-1992) doi:10.1109/IEEESTD.2014.6826459.

International Association of Classification Societies (IACS), 2019. Requirements concerning electrical and electronic installations.

International Electrotechnical Commission, 2024. Generation, transmission and distribution of electricity – operation (iec 614-01-01). URL: https://www.electropedia.org/iev/iev.nsf/display?openform&ievref=614-01-01. accessed: 2024-07-16.

Kůs, V., Peroutka, Z., Drábek, P., . Non-characteristic harmonics and interharmonics of power electronic converters, in: CIRED 2005 - 18th International Conference and Exhibition on Electricity Distribution. doi:10.1049/cp:20051030.

Li, Y., Peng, Y., Liu, F., Sidorov, D., Panasetsky, D., Liang, C., Luo, L., Cao, Y., 2017. A controllably inductive filtering method with transformer-integrated linear reactor for power quality improvement of shipboard power system. IEEE Transactions on Power Delivery 32, 1817–1827. doi:10.1109/TPWRD.2016.2574316.

Liu, Q., Liu, F., Zou, R., Wang, S., Tian, Y., Wang, Y., Yuan, L., Li, Y., 2022. A compact-design oriented shipboard power supply system with transformer integrated filtering method. IEEE Transactions on Power Electronics 37, 2089–2099. doi:10.1109/TPEL.2021.3102938.

Liu, W., Tarasiuk, T., Gorniak, M., Guerrero, J.M., Savaghebi, M., Vasquez, J.C., Su, C.L., 2018. Power quality assessment in real shipboard microgrid systems under unbalanced and harmonic ac bus voltage, in: IEEE Applied Power Electronics Conference and Exposition (APEC), pp. 521–527. doi:10.1109/APEC.2018.8341061.

Meghanathan, N., 2016. Assortativity analysis of real-world network graphs based on centrality metrics. Computer and Information Science 9, 7. doi:10.5539/cis.v9n3p7.

Milankov, R., Radić, M., 2014. Harmonics: Examples of negative impacts, in: 2014 16th International Conference on Harmonics and Quality of Power (ICHQP), pp. 435–438. doi:10.1109/ICHQP.2014.6842817.

Mindykowski, J., Tarasiuk, T., 2015. Problems of power quality in the wake of ship technology development. Ocean Engineering 107, 108–117. doi:https://doi.org/10.1016/j.oceaneng.2015.07.036.

Rahman, S., Ghering, J., Elizondo, N., Ahmad Khan, I., 2022. Intelligent filtering solutions for improving power quality in marine shipboard systems, in: IEEE Kansas Power and Energy Conference (KPEC). doi:10.1109/KPEC54747.2022.9814803.

Rigogiannis, N., Bogatsis, I., Pechlivanis, C., Terzopoulos, K., Kyritsis, A., Papanikolaou, N., Loupis, M., 2023. Power quality measurements in shipboard microgrids: A case study, in: International Conference on Electrical Drives and Power Electronics (EDPE). doi:10.1109/EDPE58625.2023.10274026.

Semwal, P., Narayanan, V., Singh, B., Panigrahi, B.K., 2022. Performance evaluation of power quality in shipboard microgrid under different working conditions, in: IEEE Global Conference on Computing, Power and Communication Technologies (GlobConPT). doi:10.1109/GlobConPT57482.2022.9938368.

Terriche, Y., Mutarraf, M.U., Mehrzadi, M., Su, C.L., Guerrero, J.M., Vasquez, J.C., Kerdoun, D., Alonso, A., 2019. Power quality and voltage stability improvement of shipboard power systems with non-linear loads, in: IEEE International Conference on Environment and Electrical Engineering and 2019 IEEE Industrial and Commercial Power Systems Europe (EEEIC / ICPS Europe). doi:10.1109/EEEIC.2019.8783356.

Tsvetanov, D., Djagarov, N., Grozdev, Z., 2023a. Improving power quality in shipboard power system using a static synchronous compensator: A simulation study, in: International Conference Automatics and Informatics (ICAI), pp. 124–132. doi:10.1109/ICAI58806.2023.10339067.

Tsvetanov, D., Milushev, H., Djagarov, N., Djagarova, J., 2023b. Investigation of power quality using a laboratory experimental setup of a shipboard power plant, in: International Conference Automatics and Informatics (ICAI), pp. 133–139. doi:10.1109/ICAI58806.2023.10339035.